

From the Two-Component System $\text{CBrCl}_3 + \text{CBr}_4$ to the High-Pressure Properties of CBr_4 Rafael Levit,[†] Maria Barrio,[†] Nestor Veglio,[†] Josep Ll. Tamarit,^{*,†} Philippe Negrier,[‡] Luis C. Pardo,^{†,§} Jorge Sanchez-Marcos,^{||} and Denise Mondieig[‡]

Departament de Física i Enginyeria Nuclear, E.T.S.E.I.B., Universitat Politècnica de Catalunya, Diagonal, 647, 08028 Barcelona, Catalonia, Spain, Centre de Physique Moléculaire, Optique et Hertzienne, UMR 5798 au CNRS-Université Bordeaux I, 351, cours de la Libération, 33405 Talence Cedex, France, Forschungsneutronenquelle Heinz Maier-Leibnitz (FRM II), Technische Universität München, Lichtenbergstraße 1, D-85747 Garching b. München, Germany, and Institut Laue Langevin, 6 Rue Jules Horowitz, Boîte Postale 156x, F-38042 Grenoble Cedex 9, France

Received: July 13, 2008; Revised Manuscript Received: September 3, 2008

The experimental phase diagram of the $\text{CBrCl}_3 + \text{CBr}_4$ system has been determined by means of X-ray powder diffraction and thermal analysis techniques from 200 K to the liquid state. Before melting, the two components have the same orientationally disordered (OD) face-centered cubic phase, and solid–liquid equilibrium is explained by simple isomorphism. The application of multiple crossed isopolymorphism formalism to the low-temperature solid–solid equilibria has enabled the inference of an OD rhombohedral metastable (at normal pressure) phase for CBr_4 . Experimental determination of the pressure–volume–temperature and construction of the pressure–temperature phase diagrams for CBr_4 reveal the existence of a high-pressure phase, the rhombohedral symmetry of which is inferred by means of the thermodynamic assessment of the experimental phase diagram and demonstrated by means of high-pressure neutron diffraction measurements. The procedure used in this work confirms the connection between the appearance of metastable phases at normal pressure and their existence at high-pressure.

1. Introduction

One of the major challenges of solid-state chemical physics in this century is to improve our ability to predict and control the appearance of different crystalline forms of a substance, the so-called “polymorphs”.^{1–5} Such a limited capability has strong consequences on technological advances and commercial progress in many fields from materials science, including pharmaceutical development, optoelectronics, to biological systems.^{3,5,6} In order to understand the complex thermodynamic and structural behavior of materials, classical studies are based on the temperature as a variable, although the pressure has appeared as a desirable tunable variable to increase the landscape of the strategies to be developed for our global understanding of polymorphism problem.^{6–8} Although impressive technological advances in high-pressure experimental devices have enabled us to gain a new understanding of the polymorphism and related subjects as pressure-induced amorphization,^{9,10} many of the new techniques are conducted in the very high-pressure domain ranged from some megabar (0.1 GPa) to pressures as high as several hundreds of GPa. Such a pressure domain is especially interesting for metals, semiconductors, superconductors or minerals, but in general exceeds for pharmaceutical or biological compounds, in general, organics, for which 1 GPa is rather a limiting pressure for the involved molecules. For these compounds polymorphism plays a key role for bioavailability or regulatory rules and economical consequences related to intellectual property.¹ Nevertheless, it should be noticed that works

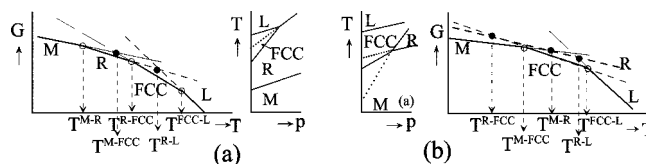


Figure 1. Gibbs energy (G) versus temperature (T) at normal pressure with the scheme of the temperature–pressure diagrams involving stable (continuous lines) and metastable (dotted lines) two-phase equilibria involving liquid (L), OD fcc and R and ordered (M) phases for (a) CBrCl_3 ¹⁶ and (b) CBr_4 ^{14,15} compounds. The empty and filled circles in the G – T diagrams denote stable and metastable phase transitions (at normal pressure), respectively.

“merging” pressure and temperature intensive thermodynamic variables are not yet a typical thermodynamic landscape scenario to describe the polymorphism of organic materials.

This paper concerns mainly the archetypical carbon tetrabromide (CBr_4) compound. Under its saturated vapor pressure, CBr_4 displays two forms: the monoclinic low-temperature phase and a high-temperature orientationally disordered (OD, or plastic) face-centered cubic (fcc) phase.^{11–13} At high but moderate pressures, Bridgman showed the existence of one additional phase (see pressure–temperature phase diagram and Gibbs energy at normal pressure in Figure 1b),^{14,15} the symmetry of which is still unknown.

On the frame of the halogenomethane series, $\text{CBr}_{4-n}\text{Cl}_n$, $n = 0, \dots, 4$, to which CBr_4 belongs, members with $n = 4$ and $n = 3$ display an OD rhombohedral (R) stable phase under its saturated pressure.^{17,16} The phase behavior at normal pressure is described in Figure 1a by means the Gibbs energy function as a function of temperature for $n = 3$. For $n = 2$, the phase behavior is virtually the same (under its saturated pressure) than for CBr_4 , and it has been recently shown the existence of a OD R phase

* To whom correspondence should be addressed. Phone: +34 93401 65 64. Fax: +34 93401 18 39. E-mail: jose.luis.tamarit@upc.edu.

[†] Universitat Politècnica de Catalunya.

[‡] UMR 5798 au CNRS-Université Bordeaux I.

[§] Technische Universität München.

^{||} Institut Laue Langevin.

appears at moderate pressures (the triple point [L + R + fcc] being located at 104.1 MPa and 320.9 K).¹⁸ It means then that for all of these compounds with the exception of CBr₄, two OD phases with fcc and R lattice symmetry can be found either under saturated pressure or at high-pressure, independently of the molecular size or molecular symmetry (T_d or C_{3v} or C_{2v}).¹⁹ This conclusion makes sense to suspect the existence of an OD R phase also for CBr₄. For this compound a high number of molecular dynamics simulation^{20–22} and experimental works^{11–13,23–27} have been published, but concerning the high-pressure field only the pioneer work of Bridgman^{14,15} and some high-pressure Raman studies and thermal conductivity measurements are known.^{28,29}

The aim of this work is two-fold. On the one hand, to characterize the polymorphism of CBr₄ as a function of temperature and pressure (up to 300 MPa); on the second hand, to infer the lattice symmetry of the high-pressure phase by means of a connection between normal-pressure properties derived from the thermodynamic analysis of the CBrCl₃ + CBr₄ two-component system and high-pressure properties of pure components. This procedure should be understood as a methodology which provides a thermodynamic path for a global understanding of the polymorphism of pure compounds (as a function of temperature and pressure) and the phase equilibria appearing in two-component systems at saturated pressure, two “worlds” rarely connected.³⁰

2. Experimental Section

2.1. Materials. CBr₄ and CBrCl₃ compounds were obtained from Fluka and Across with purity of 99%, and used as received since the measured phase transition and melting points agreed well with those previously reported.^{13–16,20,25,26}

Two-component mixtures were prepared from the melt of the materials in the selected proportions and fast cooling to room temperature.

2.2. Thermal Analysis. Thermal analyses at normal pressure were carried out by means of a Q100 from TA-Instruments using heating and cooling scanning rates of 2 K·min⁻¹ and ca. 20 mg sample masses hermetically sealed into aluminum crucibles under a controlled N₂ atmosphere.

2.3. X-ray Powder Diffraction. High-resolution X-ray powder diffraction profiles were recorded by means of a vertically mounted INEL cylindrical position-sensitive detector (CPS120). The detector was used in the Debye–Scherrer geometry (transmission mode), enabling a simultaneous recording of the profile over a 2θ range between 4 and 120° (angular step ca. 0.029°(2 θ)). Monochromatic Cu K α 1 radiation ($\lambda = 1.54059$ Å) was selected with asymmetric focusing incident-beam curved quartz monochromator. The generator power was set to 35 kV and 35 mA. As recommended, external calibration to convert the measured 4096 channels to 2θ -degrees using Na₂Ca₂Al₂F₄ cubic phase was applied by means of cubic spline fittings.³¹ The peak positions were determined after pseudo-Voigt fitting by using DIFFRACTINEL software.

Low-temperature measurements were achieved with a liquid nitrogen 700 series Cryostream Cooler from Oxford Cryosystems.

Liquid or powder samples were placed into Lindemann capillaries (0.3 or 0.1 mm diameter for mixed crystals and pure CBr₄, respectively) at room temperature. During data collection, capillaries were rotated perpendicularly to the X-ray beam direction to minimize possible effects of preferred orientations.

2.4. pVT Measurements. Density of CBr₄ as a function of pressure was isothermally measured from 328 to 400 K and up to 300 MPa with a resolution of 10⁻⁴ g·cm⁻³. Measurements were conducted by means of a homemade pVT apparatus coming

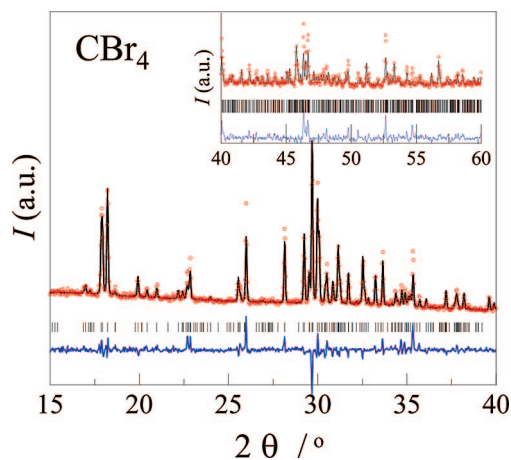


Figure 2. Experimental (O) and theoretical (-) diffraction patterns of phase M ($C2/c$) for CBr₄ at $T = 230$ K along with the difference profile (lower curve). The intensity of the inset is magnified 4 times.

from the laboratory of Professor Dr. A. Würflinger (Ruhr-Universität, Bochum, Germany). Details of the experimental system and procedures have been previously reported.^{18,30,32}

2.5. High-Pressure Neutron Diffraction Measurements.

Patterns of CBr₄ at high-pressure were collected by means of the high-flux D1B two-axis diffractometer at the Institut Laue-Langevin (Grenoble), which span a 2θ range of 70° with a wavelength of $\lambda = 2.52$ Å, as determined by calibration using a Al₂O₃ sample. Powdered CBr₄ was placed into a cylindrical (6.08 mm inner diameter and 57.4 mm inner height) high-pressure cell made of copper–beryllium and compressed at room temperature within an Orange cryofurnace which works between 1.5 and 550 K. Helium was used as a pressure transmitting medium and a piston placed at the upper part of the cell avoided the contact with sample. Temperature and pressure were controlled to measure in the desired pressure-temperature region concerning the new high-pressure phase. Low-resolution patterns (0.20° 2θ angular step) in the 10–80 2θ degrees were obtained in the 300–490 K temperature domain. Data analysis for the patterns was conducted in an analogous way that for those obtained at normal pressure.

3. Results

3.1. Characterization of Materials. 3.1.1. CBr₄. The crystal structure of the low-temperature phase was early determined by means of a single crystal study as monoclinic (space group $C2/c$ with $Z = 32$).¹¹ At 319.3 ± 1.0 K, CBr₄ transforms to a high temperature OD fcc phase.^{12,33}

X-ray powder diffraction experiments as a function of temperature were carried out from 100 K up to the liquid state. Lattice parameters of the low-temperature M phase were refined by applying Rietveld profile refinements by means of the FullProf program³⁴ on the basis of the proposed structure¹¹ as well as by a rigid molecule approach, which was proved to be valid for CBr₄ after the work of Zielinski et al.²² Figure 2 shows the experimental and calculated profiles together with the difference between them. The monoclinic lattice parameters agree quite well with those previously published.^{11,33} At 290.0 K, they have been determined to be $a = 21.3925(8)$ Å, $b = 12.1090(4)$ Å, $c = 20.9917(7)$ Å, and $\beta = 110.915(2)^\circ$. The refined lattice parameters were fitted as a function of the temperature using standard least-squares methods for each parameter. The agreement between the calculated and experimental values has been accounted by the reliability factor, defined as $R = \sum (y_o - y_c)^2 / y_c^2$, where y_o and y_c stand for the

TABLE 1: Polynomial Equations $p = p_0 + p_1T + p_2T^2$ (T in K and p in Å or in Degree (°) for β Parameter) to Which the Lattice Parameters of the Monoclinic (C2/c) and Cubic (fcc) Were Fitted As a Function of Temperature; R Is the Reliability Factor

phase	temperature range	parameter	p_0	$p_1 \times 10^3$	$p_2 \times 10^5$	$R \times 10^7$
M (C2/c)	90–320	a	20.947(5)	0.62(5)	0.32(1)	4
		b	11.768(3)	0.65(3)	0.186(9)	7
		c	20.543(7)	0.58(7)	0.34(2)	5
		β	111.66(2)	-1.9(3)	-0.26(6)	3
fcc	323–360	a	8.272(17)	1.77(5)		1

TABLE 2: Transition Temperatures T_c and Enthalpy (ΔH) and Entropy Changes (ΔS) Derived from DSC Calorimetric Measurements, Volume Changes Determined from X-ray Powder Diffraction Measurements (Δv^{XR}) and from High-Pressure pvT Measurements (Δv^{HP}), Slope of the Pressure–Temperature Two-Phase Equilibria Derived from the Application of the Clausius–Clapeyron Equation (dT_c/dp^{CC}) at Normal Pressure and Read from pvT Diagram (dT_c/dp^{exp}) of the CBr_4 ^a

property	CBr_4			
	M \rightarrow fcc	fcc \rightarrow L	M \rightarrow R	R \rightarrow fcc
T_c/K	319.2	366.2	357.6 ^b _e	217.2 ^b _e
$\Delta H/\text{kJ}\cdot\text{mol}^{-1}$	320.0 ^c , 320 ^d	363.2 ^c , 367.4 ^d	6.09 ^b	4.23 ^b
	6.51	3.56		
$\Delta S/\text{J}\cdot\text{mol}^{-1}\cdot\text{K}^{-1}$	5.94 ^c , 6.61 ^d	3.95 ^c , 3.57 ^d	17.03 ^b	1.95 ^b
	20.39	9.72		
$\Delta v^{\text{XR}} (p = 0.1 \text{ MPa})/\text{cm}^3\cdot\text{mol}^{-1}$	18.56 ^c , 20.66 ^d	10.88 ^c , 9.72 ^d		
$\Delta v^{\text{HP}} (p = 0.1 \text{ MPa})/\text{cm}^3\cdot\text{mol}^{-1}$	7.01 \pm 0.05	4.40 \pm 0.07		1.51 \pm 0.19 ^e
$(dT_c/dp)^{\text{CC}}/\text{K}\cdot\text{MPa}^{-1}$	7.13 \pm 0.20	4.22 \pm 0.23		0.774 \pm 0.050
$(dT_c/dp)^{\text{exp}}/\text{K}\cdot\text{MPa}^{-1}$	0.34 \pm 0.02	0.43 \pm 0.03	0.148 \pm 0.030	0.778 \pm 0.031
	0.313 \pm 0.003	0.345 \pm 0.015		
property	CBrCl_3			
	M \rightarrow R	R \rightarrow fcc	fcc \rightarrow L	R \rightarrow L
T_c/K	238.19	259.3	267.9	
$\Delta H/\text{kJ}\cdot\text{mol}^{-1}$	4.58	0.515	2.03	2.55
$\Delta S/\text{J}\cdot\text{mol}^{-1}\cdot\text{K}^{-1}$	19.23	1.98	7.61	9.58
$\Delta v^{\text{XR}} (p = 0.1 \text{ MPa})/\text{cm}^3\cdot\text{mol}^{-1}$	4.31 \pm 0.40	1.41 \pm 0.30	2.72	
$\Delta v^{\text{HP}} (p = 0.1 \text{ MPa})/\text{cm}^3\cdot\text{mol}^{-1}$	4.20 \pm 0.55	1.41 \pm 0.12	2.82 \pm 0.14	3.65 \pm 0.43
$(dT_c/dp)^{\text{CC}}/\text{K}\cdot\text{MPa}^{-1}$	0.218	0.714	0.357	0.380
$(dT_c/dp)^{\text{exp}}/\text{K}\cdot\text{MPa}^{-1}$	0.217 \pm 0.009	0.61 \pm 0.04	0.38 \pm 0.01	0.35 \pm 0.01

^a M refers to the low-temperature monoclinic (C2/c) phase, and R and fcc for the OD rhombohedral and face-centered cubic phases, respectively. Data for CBrCl_3 are taken from ref 16. ^b Values obtained by extrapolation of the [M + R] equilibrium of the $\text{CBrCl}_3 + \text{CBr}_4$ two-component system and, for temperatures, also extrapolated from the p–T phase diagram (^e). ^c Reference 25. ^d Reference 13. ^e Average of the experimental high-pressure values.

measured and calculated lattice parameters, respectively. Table 1 gathers the coefficients of the polynomial equations and Figure 3 depicts both experimental values and polynomials for the monoclinic phase.

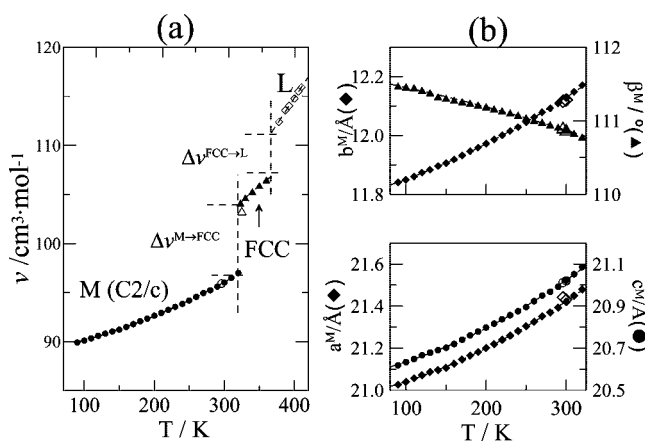


Figure 3. Molar volume of CBr_4 as a function of temperature (at normal pressure) derived from X-ray diffraction experiments for the solid phases and from pvT measurements for the liquid phase. (b) Monoclinic lattice parameters as a function of temperature. Filled symbols correspond to values previously published for the M^{11,33} and fcc¹² phases.

As far as the OD fcc phase is concerned, lattice parameters were refined according to the pattern matching option of FullProf. Lattice parameters of the OD fcc phase were found to match literature data, although the scattering of data is considerable higher than for the low-temperature phase. Nevertheless, the higher differences are ca. 0.8%.^{12,23,24}

The molar volume, calculated from the lattice parameters as a function of temperature, is represented in Figure 3. These values, together with the density of the liquid phase at normal pressure, enable to determine the volume changes at the phase transitions (see Table 2).

As for high-pressure measurements, density was measured as a function of pressure (up to 300 MPa) for a representative number of isotherms (Figure 4a). Such a pvT phase diagram enables us (i) to determine the volume changes at the phase transitions (Figure 4b) and (ii) to build up the pressure-temperature (pT) phase diagram (see inset in Figure 4a). From the high-pressure measurements it clearly emerges the appearance of a high-pressure phase, the symmetry of which will be demonstrated in the next section (related to the $\text{CBrCl}_3 + \text{CBr}_4$ two-component system) as OD rhombohedral (R) phase. The coexistence of the M and OD R and fcc phases (triple point) is found at 221.6 MPa and 390.0 K. Topologically the pT phase diagram matches quite well with that determined long time ago from Brigmann.^{14,15} According to the slopes of the determined

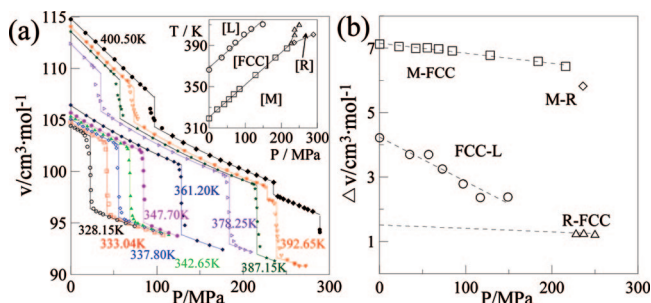


Figure 4. (a) Molar volume as a function of pressure for several temperatures and, as an inset, the pressure-temperature phase diagram for CBr₄. (b) Volume changes for the melting and solid–solid phase transitions as a function of pressure.

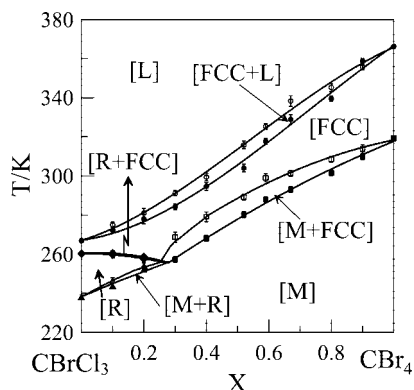


Figure 5. Experimental CBrCl₃ + CBr₄ phase diagram.

two-phase equilibria, it can also be inferred an additional triple point beyond the analyzed experimental pressure and temperature domain sharing fcc, R and L phases at (321.2 MPa, 467.0 K), which implies the disappearance of the OD fcc phase at high pressures. It should be noticed that for CBr₂Cl₂, the pT phase diagram was found to be the same from a topological point of view.¹⁸

3.1.2. CBrCl₃. The polymorphism of CBrCl₃ at normal and at high pressure has been recently studied.¹⁶ The lattice symmetry of low-temperature ordered phase is C2/c ($Z = 32$). In a recent work it has been clearly established the isostructural character of the low-temperature ordered monoclinic phase for all the halogenomethane compounds of the family CBr_{4-n}Cl_n, $n = 0, \dots, 4$.³⁵

At 238.1 K the monoclinic phase transforms to an OD R phase. At 260.3 K a new OD fcc phase appears, which is stable up to the melting point at 267.1 K. It should be noticed that for the CBr₂Cl₂, CBrCl₃, and CBr₄ compounds, the high-pressure behavior is topologically similar in relation to the behavior of the OD fcc: at high-pressure this phase disappears beyond the [fcc + R + L] triple point, irrespective of the existence of the OD R phase at normal pressure which is only present for CCl₄ and CBrCl₃.¹⁹

3.2. Two-Component System. 3.2.1. Thermal Analysis. Accurate transition and melting temperatures and related enthalpy changes were determined by means of thermal analysis. To ensure the sequence of stable phases, samples were slowly cooled from room temperature to about 190 at 2 K·min⁻¹ and heated back to the liquid state. The obtained temperature-composition data were used to construct the phase diagram (Figure 5). The two-component system has a peritectic three-phase equilibrium at 256.3 K involving M, fcc, and R phases.

The heat effects associated with the solid–liquid and solid–solid phase transitions, derived from the thermal measurements, are depicted in Figure 6.

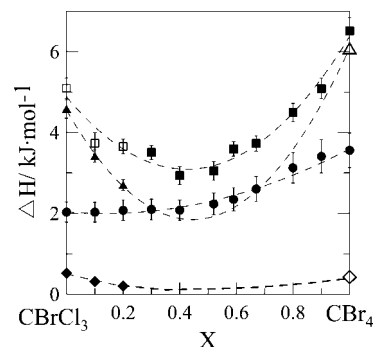


Figure 6. Experimental (full symbols) enthalpies of melting of the fcc phase (circles) and for the R to fcc (squares), M to R (triangles) and M to R (triangles) transitions as a function of the mole fraction. Empty symbols are calculated values from eq 4.

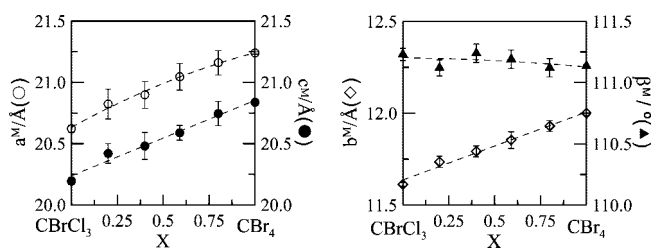


Figure 7. Monoclinic lattice parameters as a function of mole fraction at $T = 230$ K.

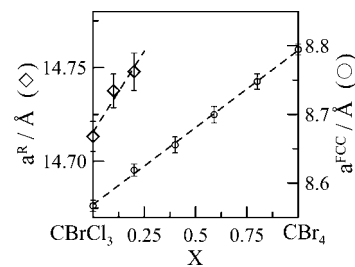


Figure 8. Lattice parameter a^R for the OD R mixed crystals at 258 K (α parameter is not shown because it remains almost constant) and a^{fcc} for OD fcc mixed crystals extrapolated at 290 K as a function of the mole fraction.

3.2.2. Crystallographic Characterization. Monoclinic Mixed Crystals. Although it has been shown that monoclinic phases for all the compounds of the halogenated compounds are isostructural,³⁵ continuous formation of mixed crystals as a function of composition has been verified at 230 K. It should be noticed that the monoclinic lattice parameters for mixed crystals are a function of the fractional occupancy of the halogen atoms and deviate slightly from the Vegard's law, as previously described for mixed crystals between other members of the halogenomethane compounds.³⁵ This behavior is a direct consequence of the statistical disorder of the averaged molecule in the monoclinic mixed crystals in such a way that sites have a fractional occupancy of Cl and Br atoms directly coupled to the composition of the mixed crystal.

Rhombohedral Mixed Crystals. X-ray powder diffraction was conducted at 258 K for several samples with $X \leq 0.2$ in order to well define the R phase for the mixed crystals. Lattice parameters for such a domain are depicted in Figure 8.

Face-Centered Cubic Mixed Crystals. X-ray diffraction patterns of the fcc mixed crystals were obtained for the whole concentration range by slow cooling of the liquid mixtures. Because there is not a common temperature for which all the mixed cubic crystals can be found (stable or metastable), X-ray measurements were performed for several compositions as a

function of temperature and thereafter determined lattice parameters were extrapolated at 290 K. As can be seen (Figure 8), the lattice parameter of the fcc mixed crystals evolves continuously from $X = 0$ to $X = 1$, thus making evident the existence of an isomorphism relationship between cubic phases of both compounds.

3.2.3. Thermodynamic Analysis Procedure. For the sake of completeness, we sketch here the required basis on the thermodynamic analysis based on the crossed isopolymorphism. Details can be found in previous works.^{36–38}

Each phase α of a two-component mixture of composition X , $A_{1-X}B_X$, can be described under isobaric conditions by a molar Gibbs energy function, $G^\alpha(T, X)$, which provides all the thermodynamic information, the equilibrium condition being fulfilled when the total Gibbs energy reaches its lowest value. Thus, at a given T , when two Gibbs energy curves for two different phases intersect, there will be a pair of coexisting phases.

The molar function of the Gibbs energy of phase α is given by the following function of T and X :

$$G^\alpha(T, X) = (1 - X)\mu_A^{*,\alpha} + X\mu_B^{*,\alpha} + RTLN(X) + G^{E,\alpha}(T, X) \quad (1)$$

where $\mu_i^{*,\alpha}$, $i = A, B$, represent the molar Gibbs energies of pure components A and B, R is the gas constant, $LN(X) = (1 - X)\ln(1 - X) + X\ln X$ and $G^{E,\alpha}(T, X)$ is the excess Gibbs energy that accounts for the deviation of the mixture in phase α from ideal mixing behavior.

The two-phase equilibrium region between α and β phases will be given by the common tangent rule between their respective Gibbs energies, $G^\alpha(T, X)$ and $G^\beta(T, X)$ at each T . Because of the lack of data on $\mu_i^{*,j}$, $i = A, B$, and $j = \alpha, \beta$, the equal Gibbs curve (EGC) method provides the difference between the Gibbs energies of the α and β phases as

$$\Delta_\alpha^\beta G(T, X) = G^\beta(T, X) - G^\alpha(T, X) = (1 - X)\Delta_\alpha^\beta \mu_A^*(T) + X\Delta_\alpha^\beta \mu_B^*(T) + \Delta_\alpha^\beta G^E(T, X) \quad (2)$$

where $\Delta_\alpha^\beta \mu_i^*(T)$ is $\mu_i^{*,\beta} - \mu_i^{*,\alpha}$ ($i = A, B$) and $\Delta_\alpha^\beta G^E(T, X)$ is the excess Gibbs energy difference between the considered phases, that is, $G^{E,\beta}(T, X) - G^{E,\alpha}(T, X)$.

Assuming $\Delta_\alpha^\beta \mu_i^*(T) \approx \Delta_\alpha^\beta S_i(T_i^{\alpha-\beta} - T)$, where $\Delta_\alpha^\beta S_i$ and $T_i^{\alpha-\beta}$ are the entropy change and temperature for the $\alpha \rightarrow \beta$ transition, the equation $\Delta_\alpha^\beta G(T_{EGC}, X) = 0$ provides a curve (EGC curve) where phases α and β have equal values for the Gibbs energies, which is described by the following equation:

$$T_{EGC}(X) = \frac{(1 - X)\Delta_\alpha^\beta H_A + X\Delta_\alpha^\beta H_B}{(1 - X)\Delta_\alpha^\beta S_A + X\Delta_\alpha^\beta S_B} + \frac{\Delta_\alpha^\beta G^E(X)}{(1 - X)\Delta_\alpha^\beta S_A + X\Delta_\alpha^\beta S_B} \quad (3)$$

where $\Delta_\alpha^\beta H_i$ is the transition enthalpy for component i .

Using the experimental data of equilibrium [$\alpha + \beta$], the excess Gibbs energy difference close to the EGC curve, $\Delta_\alpha^\beta G^E(X)$, is obtained; in addition, the coherence of the full phase diagram is achieved by combining the Gibbs function of the involved phases.

As for the [fcc + L] equilibrium the evidence of the isomorphism relationship between the stable fcc phases of

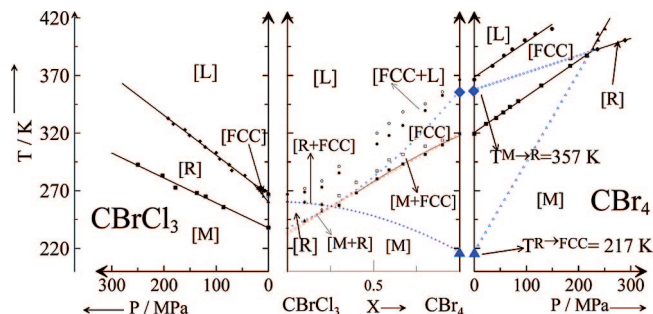


Figure 9. Center panel: Calculated two-phase equilibria for the two-component system $CBrCl_3 + CBr_4$ at normal pressure (red lines) together with the extrapolated equilibria from the thermodynamic assessment (blue lines). Left and right panels show the pressure–temperature phase diagrams of the $CBrCl_3$ and CBr_4 compounds, respectively. Dotted blue lines correspond to the extrapolation of the high-pressure two-phase equilibria at normal pressure.

$CBrCl_3$ and CBr_4 as demonstrated by the continuity of the (T, X) loop and of the lattice cubic parameter (continuous formation of mixed crystals), thermodynamic assessment can be easily done (Figure 9) by applying eq 3 for $\alpha = fcc$ and $\beta = L$. The experimental temperature and enthalpy and entropy changes of the pure compounds can be found in Table 2.

Concerning the [R + fcc], [M + fcc] and [M + R] two-phase equilibria, the crossed isopolymorphism concept should be recalled. It entails for each phase of component A (or B) the existence of an isomorphous (metastable) phase for component B (or A). Thus, extension of the [M + R] and [R + fcc] loops at $X = 1$ and the [M + fcc] at $X = 0$ provide the metastable phase transitions M to R and R to fcc for CBr_4 and, similarly, from M to fcc for $CBrCl_3$. These extrapolations concerning temperatures are indicated in Figure 9 and the physical meaning is shown in Figure 1 (see filled circles in the Gibbs energy functions as a function of temperature). It should be pointed out that as the stable [R + fcc] loop extends to a maximum of about 20% of the mole fraction, extrapolating to $X = 1$, that is, the R to fcc phase transition of CBr_4 (T^{R-FCC} metastable transition in Figure 1b), would lead to a significant error. Identical argument goes along with the [M + R] loop. Nevertheless, this a priori default is balanced by the thermodynamic assessment of the complete (T, X) phase diagram in combination with extrapolated data from the pVT diagram, which reduces strongly the temperature window of the extrapolated temperature (± 5 K).

A widespread assumption is that the specific heat of the OD R and fcc phases are close and owing to the closeness of the transition (stable or metastable) temperatures, the associated enthalpy changes (Figure 6) can be related by

$$\Delta H_{q \rightarrow \gamma} = \Delta H_{q \rightarrow \alpha} + \Delta H_{\alpha \rightarrow \gamma} \quad (4)$$

which enables to expand experimental data and makes possible and physically coherent to extrapolate enthalpy changes for the metastable phase transitions (see Table 2 and Figure 6).

By using the fundamental thermodynamic properties determined for the whole of phase transitions (stable and metastable), thermodynamic assessment provides a perfect agreement between experimental and calculated phase diagrams, thus enhancing the validity of the calculated phase transition properties of pure compounds.

To confirm the symmetry of the high-pressure OD R phase of CBr_4 , several neutron diffraction measurements at around

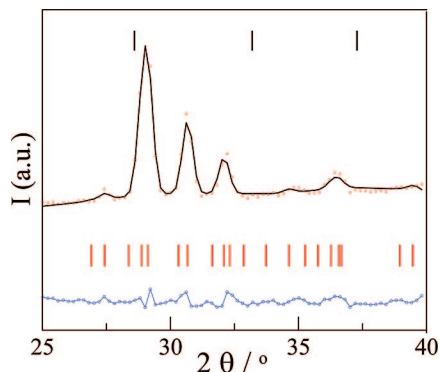


Figure 10. Experimental (red circles) and calculated (continuous black line) neutron diffraction patterns of the R phase for CBr₄ at 460 K and ca. 320 MPa along with the difference profile (bottom blue line). The vertical red bars stand for the Bragg reflections ($\lambda = 2.52 \text{ \AA}$) of the R phase (bottom red lines) and vertical top black bars for the fcc Bragg reflections for the pattern at 397 K and ca. 180 MPa, which are also shown for comparison.

300 MPa were performed. Figure 10 depicts a pattern of the OD R phase as well as the Bragg reflections for the OD phase, both at high-pressure. In spite of the low-resolution of the patterns of the high-pressure R phase, which prevents a Rietveld refinement, pattern matching procedures with the rhombohedral lattice parameters of CBrCl₃ as initial set enable to conclude irrefutably the isomorphism relationship between both R phases and, thus, to give a coherent description of the polymorphism for all the members of the halogenomethane series. The refined lattice parameters for the OD R phase of CBr₄ are $a = 15.00(3) \text{ \AA}$ and $\alpha = 88.9(1)^\circ$.

4. Discussion

The low-temperature domain of the two-component phase diagram depicted in Figure 9 has been considered as the result of interfering three solid–solid loops (crossed isopolymorphism). In general, an important part of the thermodynamic analysis when crossed isopolymorphism is involved consists in finding the metastable ends of the extrapolated loops, that is, the metastable transition points of the two pure components (see temperatures in the Gibbs energy diagrams of Figure 1).³⁸ Temperatures and enthalpy changes for those metastable points are generally determined by trial and error methods because no available experimental data exist. So, crossed isopolymorphism is widely used without any experimental physical demonstration of the existence of the generated phases for the pure components. Only for very few cases, metastable phases are known to make physical appearance. A nice example has been recently published concerning the even-numbered-carbon atoms of n-alkanes for which two-component phase diagrams described by means the concept of crossed isopolymorphism can explain the monotropic character of intermediate phases.³⁹

For the analyzed CBrCl₃ + CBr₄ two-component system, we have hypothesized that CBr₄ exhibits, in addition to the OD fcc phase, a metastable (at normal pressure) OD R phase, for which high-pressure neutron diffraction patterns clearly evidenced its real physical appearance. The temperatures and enthalpy changes between such a phase and those known to appear at normal pressure have been determined either experimentally from the extrapolation of the two-phase equilibria or from the thermodynamic assessment conducted by means the concept of crossed isopolymorphism. Figure 9 makes the connection between the results of the thermodynamic assessment and the physical meaning of the phases and phase transitions

appearing as metastable, at normal pressure, for CBr₄. It can be clearly seen that induced metastable transitions for pure compounds correspond to the extrapolated high-pressure two-phase equilibria ([M + R] and [R + fcc]). It should be then emphasized that according to the CBr₄ pT phase diagram, the extrapolation of the [M + R] equilibrium at normal pressure gives the temperature at which M phase would transform to R phase if the fcc phase would not exist and, as thermodynamically required, that such an extrapolated value falls in the temperature stability domain of the OD fcc phase at normal pressure, which strengthens the ubiquitous metastable character of the R phase at normal pressure (see Gibbs energy in Figure 1b). Analogous conclusion can be applied to the R to fcc temperature transition at normal pressure extrapolated from the [R + fcc] pressure–temperature two-phase equilibrium.

The disordered character of the OD fcc has been largely demonstrated in the past and regarding the inferred high-pressure OD R phase, several experimental evidence found in this work enable to assign such a character. On the one hand, the average volume change at the R to fcc transition in the high-pressure range (Figure 4b) is $1.258 \pm 0.014 \text{ cm}^3 \cdot \text{g}^{-1}$, a small value compatible with such a kind of transitions as demonstrated for the related compounds of the series ($1.41 \text{ cm}^3 \cdot \text{g}^{-1}$ for CBrCl₃ and $1.19 \text{ cm}^3 \cdot \text{g}^{-1}$ for CBr₂Cl₂, the last one also at high-pressure).^{16,18} The same argument can be applied for the entropy change at the R to fcc transition (see Table 2) which is lower than 2.5R, the limiting value according to Timmermanns' rule.⁴⁰ Finally, the further evidence which strongly supports the disordered character comes from the thermodynamic assessment performed for the two-component system which undoubtedly gives rise to the emergence of a new (metastable) phase for CBr₄ compound which must be isomorphous to the OD R phase for the CBrCl₃ compound, for which the physical properties have been largely proved its OD character. Although it can not be claimed as a physical argument, it can also be considered as an intuitive element placed on the domain of the chemical and physical coherence.⁴³ For the compounds belonging to the series CBr_{4-n}Cl_n, $n = 0, 2, 3$ (compound with $n = 1$ seems to be chemically unstable), it has been shown the existence of an OD R phase.^{16,19,41,42} Similar findings have been found within the (CH₃)_{4-n}CCl_n, $n = 0, \dots, 4$ series.^{36,44–46} In addition, OD R mixed crystals between such compounds are known to exist for a noticeable range of composition. We must recall that conditions ruling the formation of mixed crystals are determined from the physical properties of the involved phases, such as intermolecular interactions, size and shape of the molecules, long-range translational and orientational order, the symmetry of the crystallographic site versus the molecular symmetry of the guest molecule in the host lattice, and so forth.⁴⁷ In fact, the balance between intermolecular interactions and the steric conditions, as a whole, appears as the key requirement to stabilize a phase. Such conditions, and thus the stability of a phase, can be modified either by changing the intrinsic thermodynamic natural variables governing the phase behavior of a pure compound, temperature and pressure, or by changing the surroundings of the molecules by introducing guest molecules, that is, mixed crystals. Then it is not surprising that two-component systems (between chemical related components) and pressure–temperature phase diagrams can share the same phases because the fine-tuning of relative stability can be achieved from both “thermodynamic paths”.

Finally, it should be mentioned that one can extrapolate the pressure–temperature two-phase equilibria below “normal pressure” reaching even negative pressure values. Such an exercise

would generate some other solid–liquid, solid–solid phase transitions or even dense liquid–normal liquid transition.^{48–50}

5. Conclusions

The existence of a high-pressure phase for CBr₄ as determined by Bridgman long ago has been confirmed and, in addition, the thermodynamic properties in relation to the well-known monoclinic and OD fcc stable phases at normal pressure have been given. Owing to the thermodynamic properties such a phase has been characterized as an orientationally disordered phase the symmetry of which is rhombohedral.

The arguments for such a conclusion have been derived from the experimental pressure–volume–temperature and pressure–temperature phase diagrams of CBr₄, from the two-component system CBrCl₃ + CBr₄, and finally by high-pressure neutron diffraction measurements. The thermodynamic assessment of the two-phase equilibria of such a binary phase diagram on the basis of the crossed isopolymorphism concept provides a straightforward method to determine the metastable transition points at normal pressure. Such metastable points match perfectly with those obtained from the extrapolation at normal pressure of the high-pressure two-phase equilibria relating the same phases.

Worth recalling here is that the conclusions of the present work can be generalized whatever the chemical properties of the involved substances. Nevertheless, it is evident that the existence of mixed crystals for a noticeable domain of composition should appear in order to get reasonable two-phase equilibria making possible extrapolations as a function of composition so then the choice of the second component should be done with some constraints. This apparent strong restriction can be easily skipped when considering a series of compounds. Within the present case, the halogenomethane series CBr_{4-n}Cl_n, $n = 0, \dots, 4$ gives us a unique opportunity to show up the connection between the normal pressure two-component phase equilibria with the high-pressure properties of pure components. As the van der Waals molecular volume of the molecules in the series decreases with n , it is quite obvious that at least from steric constraints mixed crystals between CBr₂Cl₂ and CBr₄ should enlarge the probability of finding continuous formation of solid solutions. Nevertheless, the pressure–temperature phase diagram of CBr₂Cl₂ is virtually the same, from a topological point of view, than that of CBr₄. Then, it means that for the two-component phase diagram sharing CBr₂Cl₂ and CBr₄ at normal pressure OD R mixed crystals can be missed making then impossible to correlate the metastable transition points sharing OD R phase derived from a thermodynamic assessment and those extrapolated from high-pressure equilibria. This is not always the case because mixed crystals can stabilize phases which do not appear at normal pressure for pure components but do at high-pressure or for other members of the series.^{39,51}

Acknowledgment. This work was supported by the Spanish Ministry of Education and Science (MEC) under Project FIS2005-00975 and by the Catalan government by the Grant SGR2005-00535. We thank ILL and Spanish CRG-D1B for allocating neutron beam time.

References and Notes

- (1) Brittain, H. G. *J. Pharm. Sci.* **2007**, *96*, 705.
- (2) Herstein, F. H. *Cryst. Growth Des.* **2004**, *4*, 1419.
- (3) Raiteri, P.; Marton, R.; Parrinello, M. *Angew. Chem.* **2005**, *44*, 3769.
- (4) Fabiani, F. P. A.; Pulham, C. R. *Chem. Soc. Rev.* **2006**, *35*, 932.

- (5) Neumann, M. A.; Perrin, M. A. *J. Phys. Chem. B* **2005**, *109*, 15531.
- (6) McMillan, P. F. *Chem. Soc. Rev.* **2006**, *35*, 855.
- (7) McMillan, P. F. *Nat. Mater.* **2005**, *4*, 715.
- (8) McMillan, P. F. *Nat. Mater.* **2007**, *6*, 7.
- (9) Wilding, M. C.; Wilson, M.; McMillan, P. F. *Chem. Soc. Rev.* **2006**, *35*, 964.
- (10) Drozd-Rzoska, A.; Rzoska, S. J.; Paluch, M.; Roland, C. M. *J. Chem. Phys.* **2007**, *126*, 164504.
- (11) More, M.; Baert, E.; Lefebvre, J. *Acta Crystallogr.* **1977**, *B33*, 3681.
- (12) More, M.; Lefebvre, J.; Fouret, R. *Acta Crystallogr.* **1977**, *B33*, 3862.
- (13) Silver, L.; Rudman, R. *J. Phys. Chem.* **1970**, *74*, 3134.
- (14) Bridgman, P. W. *Proc. Am. Acad. Arts Sci.* **1915**, *51*, 5.
- (15) Bridgman, P. W. *Proc. Am. Acad. Arts Sci.* **1938**, *72*, 227.
- (16) Parat, B.; Pardo, L. C.; Barrio, M.; Tamarit, J. Ll.; Negrier, Ph.; Salud, J.; López, D. O.; Mondieig, D. *Chem. Mater.* **2005**, *17*, 3359.
- (17) Rudman, R.; Post, B. *Science* **1966**, *154*, 1009.
- (18) Barrio, M.; Tamarit, J. Ll.; Negrier, Ph.; Pardo, L. C.; Veglio, N.; Mondieig, D. *New J. Chem.* **2008**, *32*, 232.
- (19) Tamarit, J. Ll.; Barrio, M.; Pardo, L. C.; Negrier, Ph.; Mondieig, D. *J. Phys.: Condens. Matter* **2008**, *20*, 244110.
- (20) Dove, M. T. *J. Phys. C.: Solid State Phys.* **1986**, *19*, 3325.
- (21) Dove, M. T.; Lynden-Bell, R. M. *J. Phys. C.: Solid State Phys.* **1986**, *19*, 3363.
- (22) Zielinski, P.; Fouret, R.; Foulon, R.; More, M. *J. Chem. Phys.* **1990**, *93*, 1948.
- (23) Descamps, M. *J. Phys. (Paris)* **1984**, *45*, 587.
- (24) Foulon, G.; Descamps, M. *J. Phys. C.: Solid State Phys.* **1980**, *13*, 2847.
- (25) Frederick, K. J.; Hildebrand, J. H. *J. Am. Chem. Soc.* **1939**, *61*, 1555.
- (26) Marshall, J. G.; Staveley, L. A. K.; Hart, K. R. *Trans. Faraday Soc.* **1956**, *52*, 19.
- (27) Pettitt, B. A.; Wasylishen, R. E. *Chem. Phys. Lett.* **1979**, *63*, 539.
- (28) Andersson, P.; Ross, R. G. *Mol. Phys.* **1979**, *39*, 1359.
- (29) Adams, D. M.; Sharma, S. K. *J. Chem. Soc., Dalton Trans.* **1976**, 2424.
- (30) Jenau, M.; Reuter, J.; Würflinger, A.; Tamarit, J. Ll. *J. Chem. Soc., Faraday Trans.* **1996**, *92*, 1899.
- (31) Evain, M.; Deniard, P.; Jouanneaux, A.; Brec, R. *J. Appl. Crystallogr.* **1993**, *26*, 563.
- (32) Landau, R.; Würflinger, A. *Rev. Sci. Instrum.* **1980**, *66*, 533.
- (33) Powers, R.; Rudman, R. *J. Chem. Phys.* **1980**, *72*, 1629.
- (34) Rodriguez-Carvajal, J.; Roisnel, T.; Gonzales-Platas, J. *FullProf Suite*, April 2004 version; Laboratoire Léon Brillouin, CEA-CNRS, CEN: Saclay, France, 2004.
- (35) Negrier, Ph.; Tamarit, J. Ll.; Barrio, M.; Pardo, L. C.; Mondieig, D. *Chem. Phys.* **2007**, *336*, 150.
- (36) Pardo, L. C.; Barrio, M.; Tamarit, J. Ll.; López, D. O.; Salud, J.; Negrier, Ph.; Mondieig, D. *Phys. Chem. Chem. Phys.* **2001**, *3*, 2644.
- (37) Salud, J.; López, D. O.; Barrio, M.; Tamarit, J. Ll. *J. Mater. Chem.* **1999**, *9*, 909.
- (38) Oonk, H. A. J.; Tamarit, J. Ll. *Measurement of Thermodynamic Properties of Multiple Phases, Experimental Thermodynamics*; Weir, R. D., de Loos, T. W., Eds.; (IUPAC), Elsevier: Amsterdam, 2005; Vol. VII, Chapter 9.
- (39) Espeau, P.; Céolin, R. *J. Phys. Chem. B* **2008**, *112*, 2063.
- (40) Timmermans, J. *J. Phys. Chem. Solids.* **1961**, *18*, 1.
- (41) Barrio, M.; Negrier, Ph.; Pardo, L. C.; Tamarit, J. Ll.; Mondieig, D. *J. Phys. Chem. B* **2007**, *111*, 8899.
- (42) Barrio, M.; Pardo, L. C.; Tamarit, J. Ll.; Negrier, Ph.; López, D. O.; Salud, J.; Mondieig, D. *J. Phys. Chem. B* **2006**, *110*, 12096.
- (43) Reuter, J.; Büsing, D.; Tamarit, J. Ll.; Würflinger, A. *J. Mater. Chem.* **1997**, *7*, 41.
- (44) Pardo, L. C.; Parat, B.; Barrio, M.; Tamarit, J. Ll.; López, D. O.; Salud, J.; Negrier, Ph.; Mondieig, D. *Chem. Phys. Lett.* **2005**, *402*, 408.
- (45) Pardo, L. C.; Barrio, M.; Tamarit, J. Ll.; Salud, J.; López, D. O.; Negrier, Ph.; Mondieig, D. *Phys. Chem. Chem. Phys.* **2004**, *6*, 417.
- (46) Pardo, L. C.; Barrio, M.; Tamarit, J. Ll.; López, D. O.; Salud, J.; Negrier, Ph.; Mondieig, D. *J. Phys. Chem. B* **2001**, *105*, 10326.
- (47) Barrio, M.; López, D. O.; Tamarit, J. Ll.; Negrier, Ph.; Haget, Y. *J. Mater. Chem.* **1995**, *5*, 431.
- (48) Imre, A. R.; Van Hook, W. A. *Chem. Soc. Rev.* **1998**, *27*, 117.
- (49) Imre, A. R.; Drozd-Rzoska, A.; Kraska, T.; Rzoska, S. J.; Wojciechowski, K. W. *J. Phys.: Condens. Matter* **2008**, *20*, 244104.
- (50) Imre, A. R. *Phys. Status Solidi B* **2007**, *244*, 893.
- (51) Barrio, M.; Font, J.; López, D. O.; Muntasell, J.; Tamarit, J. Ll.; Chanh, N. B.; Haget, Y. *J. Phys. Chem. Solids* **1991**, *52*, 665.